ICIC Express Letters
Volume **16**, Number **9**, September **2022**

ICIC International ©2022 ISSN 1881-803X
pp. **983–991**

AN ADAPTIVE FRACTIONAL-ORDER SLIDING MODE CONTROL FOR VIRTUAL SYNCHRONOUS GENERATOR IN MICROGRID

Qi Teng, Dezhi Xu* and Weilin Yang

School of Internet of Things Engineering
Jiangnan University
No. 1800, Lihu Avenue, Wuxi 214122, P. R. China
6191915020@stu.jiangnan.edu.cn; wlyang@jiangnan.edu.cn
*Corresponding author: xudezhi@jiangnan.edu.cn

Received January 2022; accepted March 2022

Abstract. *When grid-connected inverters are connected to the grid, the lack of physical inertia along with low output impedance leads to large current shocks that make the system unstable. Therefore, a nonlinear control method is proposed in this paper to enable the grid-connected inverter to switch freely between grid-connected and islanding modes. The nonlinear controller is designed based on sliding mode backstepping control (SMBC). In order to improve the control accuracy, the fractional order sliding mode is constructed in the sliding mode design process. Also, considering the parameter uncertainties in the model, the unknown parameters are estimated in real time by applying an adaptive method based on the projection operator in the control system. Then the stability of the control system is proved by Lyapunov stability criterion. The simulation results show that the method has good compensation performance and strong robustness compared with other control methods.*

Keywords: Fractional-order control, Sliding mode control, Microgrid, Virtual synchronous generator

1. **Introduction.** In recent years, with the rapid development of renewable new energy generation systems such as solar energy and wind energy, the application scale of distributed energy has gradually increased, and connected to the grid through grid connected inverter. However, it has some unstable disadvantages such as intermittent and large fluctuation. Compared with traditional synchronous generators, power electronic equipment is usually lack of inertia and damping, the large number of access to the grid will further reduce the rotation of the grid backup, thus threatening the safe and stable operation of the grid [1].

Therefore, VSG control is widely concerned for its frequency modulation and voltage regulation characteristics, moment of inertia and voltage source characteristics [2]. By introducing the mechanical and electromagnetic equations of synchronous generator and simulating the external characteristics of synchronous generator, the virtual inertia and primary frequency can be adjusted to increase the virtual inertia of inverter and improve the output response quality of the system.

In fact, real synchronous generators need power system stabilizer (PSS) to suppress the oscillation of rotor excitation and restore the system balance in the shortest time. The supplementary control of voltage has adopted an additional signal added to the reference voltage excited by rotor from PSS to suppress the disturbance of oscillation [3]. Based on this idea, a new control strategy is proposed in [4-6], which is similar to the rotor motion equation and adds a power angle feedback term. The design of control strategy adopts a typical nonlinear robust control, namely backstepping control, to imitate the behavior of PSS.

DOI: 10.24507/icicel.16.09.983

Terminal sliding mode control is a control method which can overcome system uncertainty, especially for nonlinear systems, external disturbance and parameter perturbation have strong robustness [7]. In [8], a backstepping controller combining command-filter and integral sliding mode is designed to research the MG dynamics. Using the memory and genetic characteristics of the fractional calculus operator, the introduction of the fractional order into the traditional sliding mode controller increases the flexibility of controller design and improves the control quality [9,10]. In [11], in order to stabilize the output of the track jack, a fractional-order terminal sliding mode backstepping control strategy was proposed. By changing the fractional order, the system response is optimized and the output overshoot is reduced.

Based on the nonlinear VSG system error model, this paper proposes a fractional-order terminal sliding mode controller based on the backstepping method. The projection operator is used to constrain the parameter error in the system. The contributions of the paper are mainly as follows.

1) Terminal sliding mode is used to track error status and overcome system uncertainty.

2) A novel fractional-order sliding mode controller is designed to weaken the chattering caused by traditional sliding mode control.

3) The projection operator adaptive law can estimate the system with virtual inertia and damping parameters without introducing additional parameters.

4) The controller adopts the state equation design, and uses the Lyapunov function to verify whether the system is asymptotically stable.

This paper is organized as follows. In Section 2, the mathematical model of VSG is introduced. In Section 3, the design process of the proposed control strategy is described. At the same time, the stability of the controller is analyzed. In Section 4, the feasibility of the controller is proved by simulation. In Section 5, conclusions are presented.

2. **Mathematical Model of VSG.** The main model of VSG inverter in MG is shown in Figure 1. In the figure, the resistance R_s and inductance L_s represent the stator impedance. R_g and L_g represent the line impedance. u_{ga}, u_{gb} and u_{gc} respectively represent the three-phase voltage of the power grid [12]. Among them, $\widetilde{i} = [i_a\, i_b\, i_c]^T = \left[i\cos\varphi \quad i\cos\left(\varphi - \frac{2\pi}{3}\right) \quad i\cos\left(\varphi - \frac{4\pi}{3}\right)\right]^T$ simulates the three-phase current generated by the stator. φ is current angle. $\widetilde{v} = [v_a\, v_b\, v_c]^T$ is three-phase terminal voltage. $\widetilde{e} = \psi_f \omega \widetilde{\sin}\theta$ is electromagnetic electromotive force, $\widetilde{e} = [e_a\, e_b\, e_c]^T$. ψ_f is the rotor flux. θ is voltage angle. ω is frequency. $\widetilde{\sin}\theta = \left[\sin\theta \quad \sin\left(\theta - \frac{2\pi}{3}\right) \quad \sin\left(\theta - \frac{4\pi}{3}\right)\right]^T$.

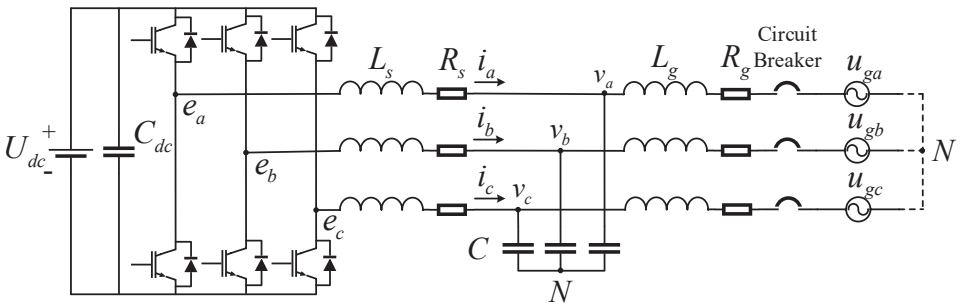

FIGURE 1. Power part of a VSG

The VSG model is shown in Figure 2. The basic concept of VSG is to introduce the rotor motion equation of SG through the control algorithm, so as to directly control the amplitude and frequency of the output voltage vector in the control, so that the inverter can simulate the external output characteristics of SG.

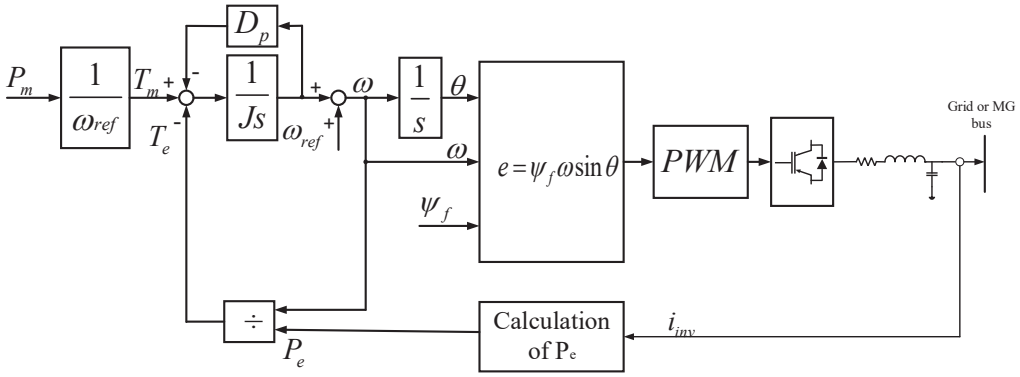

FIGURE 2. Rotor mathematical model of VSG

The equation of rotor motion of SG that is implemented in Figure 2 is given by

$$J\frac{d\Delta\omega}{dt} = T_m - T_e - D_p\left(\omega - \omega_{ref}\right) \tag{1}$$

where J stands for virtual inertia. T_m and T_e represent mechanical torque and virtual electromagnetic torque, respectively. D_p is damping coefficient, which models the effect of friction force.

The output active power can be expressed as

$$P_e = \left\langle \widetilde{i}, \widetilde{e} \right\rangle = \psi_f \omega \left\langle \widetilde{i}, \widetilde{\sin\theta} \right\rangle = \frac{3}{2}\psi_f \omega i \cos\delta \tag{2}$$

where $\delta = \theta - \varphi$ stands for power angle.

Therefore, the virtual electromagnetic torque can be obtained:

$$T_e = \frac{P_e}{\omega} = \frac{3}{2}\psi_f i \cos\delta \tag{3}$$

Similarly, the reactive power is

$$Q_e = \frac{3}{2}\psi_f \omega i \sin\delta \tag{4}$$

The design of reactive power/voltage droop control loop can be expressed as

$$V_{ref} = V_n - n\left(Q_{ref} - Q_e\right) \tag{5}$$

where V_{ref} and V_n represent voltage reference and the rated voltage, respectively. n stands for droop coefficient. Q_{ref} is reference value of reactive power.

The transfer function of the low-pass filter is

$$G_{flux}(s) = \frac{k_a}{\tau_a s + c} \tag{6}$$

Figure 3 shows the virtual flux control loop. A low-pass filter is used to simulate the SG rotor flux linkage dynamics to obtain the virtual rotor flux linkage, thereby simulating the attenuation of the synchronous motor rotor flux linkage. The attenuation of the magnetic flux of the synchronous generator is due to the application of a DC voltage on the rotor excitation, and the inductance of the rotor winding produces a delay on the stator side. In addition, due to the resistance of the rotor winding, k_a is the DC gain of the filter. The reference voltage is generated by the reactive power/voltage droop function, which is equivalent to the rotor field voltage. Therefore, in order to control the virtual rotor flux, the control signal from the controller is added to the reference voltage.

The auxiliary nonlinear controller design needs to be based on the state space model of the system [13]. Since the purpose of the auxiliary nonlinear controller is to introduce the damping torque ΔT_e, the speed deviation $\Delta\omega$ is used as a logic signal to control the VSG. The frequency deviation $\Delta\omega$ is generated by the angle controller. Therefore, the

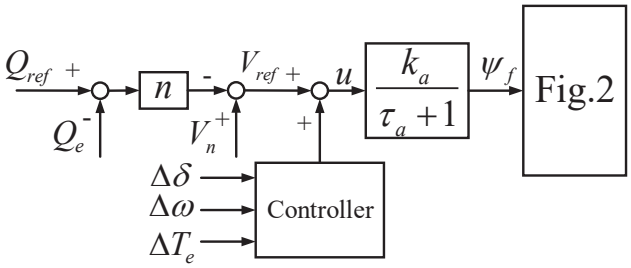

FIGURE 3. Virtual flux control diagram

power angle δ, frequency ω and electrical torque T_e are used as state variables. Therefore, their dynamics can be written as

$$\Delta\dot{\delta} = \Delta\omega \tag{7}$$

$$\Delta\dot{\omega} = -\frac{D_p}{J}\Delta\omega - \frac{1}{J}\Delta T_e \tag{8}$$

The calculation formula of torque dynamic change is

$$\dot{T}_e = \frac{3}{2}\dot{\psi}_f i\cos\delta + \frac{3}{2}\psi_f\dot{i}\cos\delta - \frac{3}{2}\psi_f i\Delta\omega\sin\delta \tag{9}$$

The flux derivative can be calculated as

$$\dot{\psi}_f = \frac{k_a}{\tau_a}u - \frac{c}{\tau_a}\psi_f \tag{10}$$

The torque can be written as

$$\dot{T}_e = \frac{3}{2}\frac{k_a}{\tau_a}ui\cos\delta - \frac{c}{\tau_a}T_e + \frac{3}{2}\psi_f\dot{i}\cos\delta - \frac{3}{2}\psi_f i\Delta\omega\sin\delta \tag{11}$$

Therefore, the perturbation form of 16 is obtained as

$$\Delta\dot{T}_e = \frac{3}{2}\frac{k_a}{\tau_a}ui\cos\Delta\delta - \frac{c}{\tau_a}\Delta T_e + \frac{3}{2}\psi_f\dot{i}\cos\Delta\delta - \frac{3}{2}\psi_f i\Delta\omega\sin\Delta\delta \tag{12}$$

Finally, the state space model of VSG system is expressed as

$$\begin{aligned}
&\Delta\dot{\delta} = \Delta\omega\\
&\Delta\dot{\omega} = \alpha\Delta\omega + \beta\Delta T_e\\
&\Delta\dot{T}_e = f_1\left(\Delta\delta, \Delta\omega, \Delta T_e\right)u + f_2\left(\Delta\delta, \Delta\omega, \Delta T_e, i, \psi_f\right)
\end{aligned} \tag{13}$$

where $\alpha = -\frac{D_p}{J}$, $\beta = -\frac{1}{J}$, $f_1\left(\Delta\delta, \Delta\omega, \Delta T_e\right) = \frac{3}{2}\frac{k_a}{\tau_a}i\cos\Delta\delta$, $f_2\left(\Delta\delta, \Delta\omega, \Delta T_e, i, \psi_f\right) = -\frac{c}{\tau_a}\Delta T_e + \frac{3}{2}\psi_f\dot{i}\cos\Delta\delta - \frac{3}{2}\psi_f i\Delta\omega\sin\Delta\delta$, u is the system control input.

3. **Controller Design.** The controller is designed for VSG based on fractional order sliding mode backstepping controller. The controller allows the states of the system to follow their desired values, ensures the stability of the system in the presence of uncertainties and disturbances, and suppresses the occurrence of oscillations. The presence of fractional order sliding modes, on the other hand, contributes to improving the control accuracy of the controller.

Since the fractional order derivative of a function may provide richer information than the integer order derivative, the fractional order calculus has been strongly developed on the basis of the integer order calculus, and different definitions of fractional order calculus have been proposed in the process, among which the definition of Riemann-Liouville fractional order calculus is more widely used in the field of fractional order calculus.

${}_{t_0}D_t^{\mu}$ is used to define the calculus operator, where $\mu \in \Re$. Riemann-Liouville definition of the μ-fold fractional order differentiation is defined as follows:

$$ {}_{t_0}D_t^{\mu} g(t) = \frac{1}{\Gamma(n-\mu)} \frac{d^n}{dt^n} \int_{t_0}^{t} \frac{g(\tau)}{(t-\tau)^{1+\mu-n}} d\tau \tag{14} $$

where $n-1 < \mu \leq n$, $\Gamma(\mu) = \int_0^{\infty} e^{-t} t^{z-1} dt$ denotes the Gamma function.

The tracking error of the system is defined as follows:

$$ \begin{aligned} e_1 &= \Delta\delta - \Delta\delta_{ref} \\ e_2 &= \Delta\omega - \Delta\omega^r \\ e_3 &= \Delta T_e - \Delta T_e^r \end{aligned} \tag{15} $$

where $\Delta\delta_{ref}$, $\Delta\omega^r$, ΔT_e^r are the reference values of the corresponding variables, respectively.

First of all, the Lyapunov function is chosen as

$$ V_1 = \frac{1}{2} {e_1}^2 \tag{16} $$

The virtual control law of the controller $\Delta\omega^r$ is optimally chosen as

$$ \Delta\omega^r = -k_1 e_1 + \Delta\dot{\delta}_{ref} \tag{17} $$

where $k_1 > 0$ is a positive constant. This virtual control law allows $\dot{V}_1 = -k_1 {e_1}^2 \leq 0$ to hold, thus ensuring the stability of the power angle δ.

And then, the fractional-order sliding mode design is performed for the angular velocity virtual controller and the torque virtual controller. The fractional order sliding mode surfaces are chosen as

$$ \begin{aligned} s_1 &= e_2 + \gamma_1 ({}_{t_0}D_t^{\mu_1} e_2)^{p_1/q_1} \\ s_2 &= e_3 + \gamma_2 ({}_{t_0}D_t^{\mu_2} e_3)^{p_2/q_2} \end{aligned} \tag{18} $$

The sliding mode reaching rate is used in the design process of the sliding mode controller, designed as follows:

$$ \begin{aligned} -c_1 \mathrm{sgn}\,(s_1) &= \dot{s}_1 \\ -c_2 \mathrm{sgn}\,(s_2) &= \dot{s}_2 \end{aligned} \tag{19} $$

where $c_1, c_2 > 0$ is a constant. It represents the rate at which the point of motion of the system converges to the switching surface $s = 0$.

The Lyapunov function is chosen as

$$ V_2 = \frac{1}{2} \left(e_1^2 + s_1^2 \right) \tag{20} $$

Therefore, the virtual control law of the controller ΔT_e^r is optimally chosen as

$$ \Delta T_e^r = \frac{1}{\beta} \left[-c_1 \mathrm{sgn}\,(s_1) - \alpha\Delta\omega + \Delta\dot{\omega}^r - \gamma_1 \left(\frac{p_1}{q_1} \right) {}_{t_0}D_t^{\mu_1} e_2 \left({}_{t_0}D_t^{\mu_1 - 1} e_2 \right)^{p_1/q_1 - 1} \right] \tag{21} $$

Consider that there may be errors in the parameters:

$$ \Delta \hat{T}_e^r = \frac{1}{\hat{\beta}} \left[-c_1 \mathrm{sgn}\,(s_1) - \hat{\alpha}\Delta\omega + \Delta\dot{\omega}^r - \gamma_1 \left(\frac{p_1}{q_1} \right) {}_{t_0}D_t^{\mu_1} e_2 \left({}_{t_0}D_t^{\mu_1 - 1} e_2 \right)^{p_1/q_1 - 1} \right] \tag{22} $$

where $\hat{\alpha}$, $\hat{\beta}$ are the parameter estimates.

This virtual control law allows $\dot{V}_2 = -k_1 {e_1}^2 - c_1 |s_1| \leq 0$, thus ensuring the stability of the angular velocity ω.

At last, the Lyapunov function is chosen as

$$ V_3 = \frac{1}{2} \left(e_1^2 + s_1^2 + s_2^2 + \frac{\tilde{\alpha}^2}{\lambda_1} + \frac{\tilde{\beta}^2}{\lambda_2} \right) \tag{23} $$

where $\tilde{\alpha} = \hat{\alpha} - \alpha$, $\tilde{\beta} = \hat{\beta} - \beta$, λ_1, λ_2 are the gains of adaptive law, so the controller u is optimally chosen as

$$u = \frac{1}{f_1(\Delta\delta, \Delta\omega, \Delta T_e)} \Bigg[-c_2 \mathrm{sgn}(s_2) - f_2(\Delta\delta, \Delta\omega, \Delta T_e, i, \psi_f) + \Delta\dot{T}_e^r - \gamma_2 \left(\frac{p_2}{q_2}\right) {}_{t_0}D_t^{\mu_2} e_3 \left({}_{t_0}D_t^{\mu_2 - 1} e_3\right)^{p_2/q_2 - 1} \Bigg] \tag{24}$$

The projection operator adaptive law can be designed as

$$\begin{aligned} \dot{\hat{\alpha}} &= \lambda_1 \mathrm{Proj}(\hat{\alpha}, s_1 \Delta\omega) \\ \dot{\hat{\beta}} &= \lambda_2 \mathrm{Proj}\left(\hat{\beta}, s_2 \Delta T_e\right) \end{aligned} \tag{25}$$

The projection operator is defined as

$$\mathrm{Proj}(\hat{\sigma}, \eta) = \begin{cases} 0 & \hat{\sigma} = \hat{\sigma}_{\max} \text{ and } \eta > 0 \\ 0 & \hat{\sigma} = \hat{\sigma}_{\min} \text{ and } \eta < 0 \\ \eta & \text{otherwise} \end{cases} \tag{26}$$

and $\mathrm{Proj}(\hat{\sigma}, \eta)$ has the conclusion as

Property1 $\hat{\sigma} \in \Omega_\sigma \triangleq \{\hat{\sigma} : \hat{\sigma}_{\min} \le \hat{\sigma} \le \hat{\sigma}_{\max}\}$

Property2 $\hat{\sigma}[\mathrm{Proj}(\hat{\sigma}, \eta) - \eta] \le 0, \forall\eta$

This control law allows $\dot{V}_3 = -k_1 {e_1}^2 - c_1 |s_1| - c_2 |s_2| \le 0$. According to Lyapunov stability condition, when $\dot{V}_3 \le 0$, the whole system will reach an asymptotically stable state by using the designed controller.

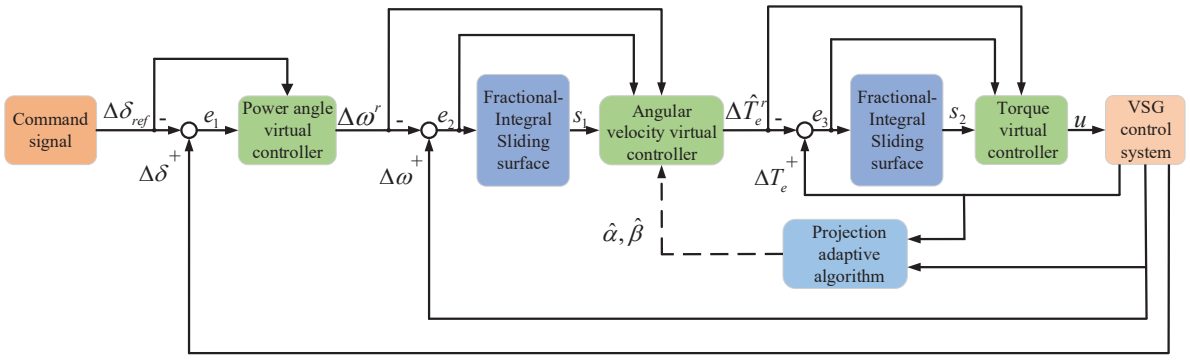

FIGURE 4. The structure of the proposed controller

4. **Main Results.** The effectiveness of the proposed control method is verified by simulation in MATLAB/Simulink.

The VSG system first operates in islanding mode, where the VSG system supplies active power to 13 kW local load. Then, the system is connected to the grid at $t = 0.3$ s, which enables the system to connect to the grid. Finally, the system is off-grid at $t = 0.7$ s to complete the transition from grid connection to islanding mode.

In the simulation, when the virtual inertia is selected as $J = 0.4$ kg·m^2 and the damping coefficient is $D = 22.5$, the rated active power is set to $P_m = 10$ kW.

Figure 5 shows a comparison of the active power variation, and it can be seen that in the islanding mode, the active power can reach the required active power quickly and smoothly. And in the active output power switching process, it is seen that the power switching under the proposed controller is smoother and the oscillation range is smaller.

Figure 6 shows the frequency variation, and it can be seen that the frequency is stable and smoother under the proposed controller, both under islanding and in grid-connected

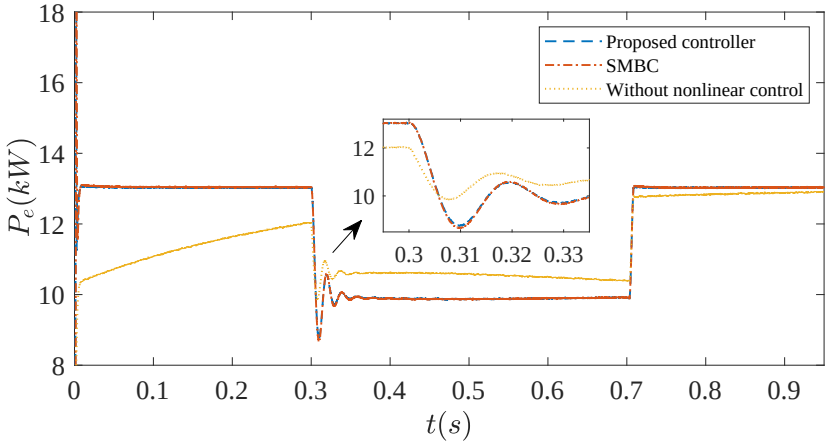

FIGURE 5. The active power variation

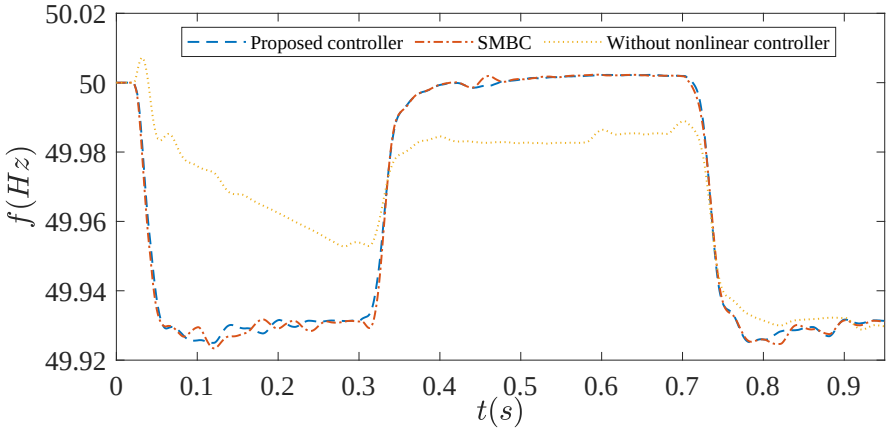

FIGURE 6. The frequency variation

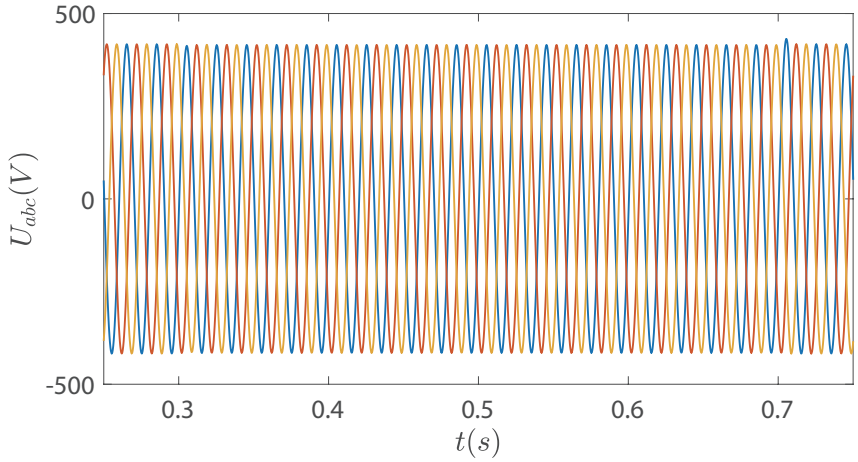

FIGURE 7. The situation of three-phase voltage of the system

operation. During switching, the frequency variation is also smoother and with less oscillation.

Figure 7 shows the three-phase voltage of the system. It can be seen that under the control of the proposed controller, the voltage waveform can be basically maintained when the system is connected to the grid and disconnected into islanding operation.

Figure 8 shows the three-phase current of the system. It can be seen that the amplitude of the phase currents decreases at $t = 0.3$ s, and the current waveforms only show slight fluctuations at the time of grid connection, after which the current waveforms are stable.

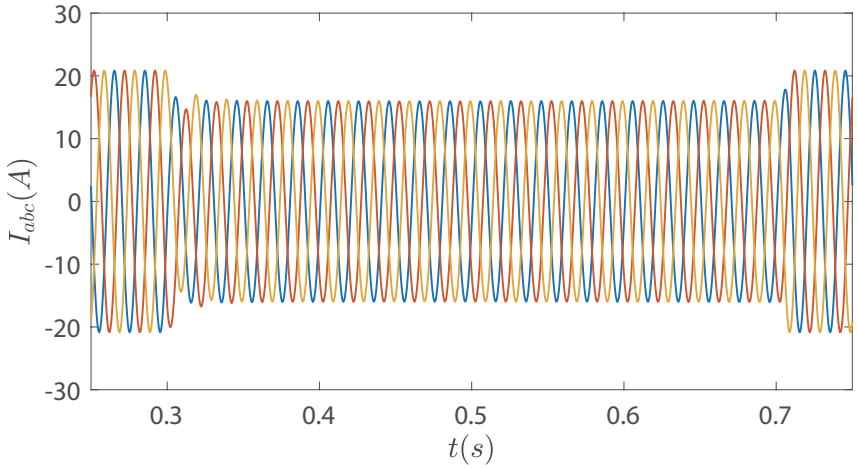

FIGURE 8. The situation of three-phase current of the system

The simulation effectively verifies that the designed controller can realize smooth switching during the transition process.

5. **Conclusions.** In this paper, a nonlinear control strategy based on the projection operator adaptive method with fractional-order sliding-mode backstepping control is proposed as a supplementary control strategy for VSG. Compared with the conventional VSG, the proposed strategy can effectively improve power damping and grid frequency tracking to cope with the intermittent and nonlinear characteristics of DG and ensure the large-signal stability of the whole system. Simulation results show that in terms of system performance, power oscillations are reduced, frequency transitions are smoother, dynamic performance and control accuracy are improved under the designed controller compared with other nonlinear and robust control methods, and the proposed controller provides a stable and flexible operation for the MG.

In the future research, we will deeply study the cooperative control of multiple VSGs based on this control strategy.

Acknowledgment. The authors gratefully acknowledge the helpful comments and suggestions of the reviewers, which have improved the presentation.

REFERENCES

[1] Y. A.-R. I. Mohamed and E. F. El-Saadany, Adaptive decentralized droop controller to preserve power sharing stability of paralleled inverters in distributed generation microgrids, *IEEE Trans. Power Electronics*, vol.23, no.26, pp.2806-2816, 2008.

[2] X. Zhang, D. B. Zhu and H.-Z. Xu, Virtual synchronous generator technology in distributed generation, *Journal of Power Sources*, pp.1-6, 2012.

[3] P. Kundur, *Power System Stability and Control*, McGraw-Hill, New York, 1994.

[4] S. M. Ashabani and Y. A.-R. I. Mohamed, A flexible control strategy for grid-connected and islanded microgrids with enhanced stability using nonlinear microgrid stabilizer, *IEEE Trans. Smart Grid*, vol.3, no.3, pp.1291-1301, 2012.

[5] S. M. Ashabani and Y. A.-R. I. Mohamed, General interface for power management of micro-grids using nonlinear cooperative droop control, *IEEE Trans. Power Systems*, vol.28, no.3, pp.2929-2941, 2013.

[6] M. Ashabani and Y. A.-R. I. Mohamed, Integrating VSCs to weak grids by nonlinear power damping controller with self-synchronization capability, *IEEE Trans. Power Systems*, vol.29, no.2, pp.805-814, 2014.

[7] K. Abidi, J. Xu and J. She, A discrete-time terminal sliding-mode control approach applied to a motion control problem, *IEEE Trans. Industrial Electronics*, vol.56, no.9, pp.3619-3627, 2009.
[8] D. Xu, G. Wang, W. Yan and X. Yan, A novel adaptive command-filtered backstepping sliding mode control for PV grid-connected system with energy storage, *Solar Energy*, vol.178, pp.222-230, 2019.
[9] S. Han, Modified grey-wolf algorithm optimized fractional-order sliding mode control for unknown manipulators with a fractional-order disturbance observer, *IEEE Access*, vol.8, pp.18337-18349, 2020.
[10] R. Hu, H. Deng and Y. Zhang, Novel dynamic-sliding-mode-manifold-based continuous fractional order nonsingular terminal sliding mode control for a class of second-order nonlinear systems, *IEEE Access*, vol.8, pp.19820-19829, 2020.
[11] L. A. Tuan, Fractional-order fast terminal back-stepping sliding mode control of crawler cranes, *Mechanism and Machine Theory*, vol.137, pp.297-314, 2019.
[12] A. Bidram and A. Davoudi, Hierarchical structure of microgrids control system, *IEEE Trans. Smart Grid*, vol.3, no.4, pp.1963-1976, 2012.
[13] A. Kanchanaharuthai and E. Mujjalinvimut, Composite nonlinear controller for higher-order models of synchronous generators under external disturbances, *International Journal of Innovative Computing, Information and Control*, vol.15, no.2, pp.465-478, 2019.